Magnetic Birefringence Study of the Electrostatic and Intrinsic Persistence Length of DNA

G. MARET, *Hochfeld-Magnetlabor des Max-Planck-Instituts für Festkörperforschung, 166X, F-38042 Grenoble Cedex, France;* and G. WEILL, *Centre de Recherche sur les Macromolecules-CNRS* and *Université L. Pasteur, Strasbourg, France*

Synopsis

Magnetic birefringence experiments were performed on solutions of DNA of intermediate molecular weight at several concentrations (c_p) over a wide range of ionic strengths (of NaCl and $MgCl_2$). The specific Cotton-Mouton constant (CM/c_p) is found to be independent of c_p when contributions from c_p to the ionic strength (μ_{eff}) are taken into account according to the concept of counterion condensation. For $\mu_{eff} \gtrsim 10^{-2}M$, CM/c_p is also independent of the ionic strength; the plateau value results in an acceptable value of the intrinsic persistence length, when a revised theoretical expression for the magnetic birefringence of wormlike chains is used, combined with new experimental data for the monomeric optical and magnetic anisotropy. For $\mu_{eff} < 10^{-2}M$, CM/c_p strongly, or weakly, increases with decreasing μ_{eff}, depending on the valency of the counterion used (Na^+ or Mg^{2+}, respectively). This increase agrees quantitatively with the variation of the electrostatic persistence length as predicted by Odijk [(1977) *J. Polym. Sci. Polym. Phys. Ed.* **15,** 477–483], Odijk and Houwaart [(1978) *J. Polym. Sci. Polym. Phys. Ed.* **16,** 627–639], and by Skolnick and Fixman [(1977) *Macromolecules* **10,** 944–948]. A comparison with other experimental data seems to reveal the importance of excluded-volume effects, which are particularly pronounced in the low-salt regime.

INTRODUCTION

The problem of DNA persistence length and of its ionic-strength dependence has been revived recently by new experimental possibilities related to the availability of samples of virtually identical molecules with very narrow length distribution[1,2] and by new theoretical advances.[3–5] Both the low- and high-ionic-strength domains present interesting problems, the former related to the general theory of polyelectrolyte solutions and the latter to understanding DNA flexibility and its relation to DNA folding in compact biological structures.

The range of salt concentrations higher than $10^{-2}M$ NaCl is easily investigated by light-scattering techniques, which give direct access to the radius of gyration.[6,7] However, this is not true at lower salt concentrations, where the q dependence of the scattered intensity is dominated by intermolecular terms in the practical range of concentrations. Most of our knowledge of the low-salt regime comes from hydrodynamic measurements such as intrinsic viscosity,[8] relaxation of electric birefringence,[9] or dichroism[10] (limited to the low-ionic-strength range because of the problem of conduction), flow birefringence,[11] or flow dichroism.[12]

Biopolymers, Vol. 22, 2727–2744 (1983)

CCC 0006-3525/83/122727-18 $02.80

It has been proposed[13] that the steady-state value of magnetic birefringence, i.e., the specific Cotton-Mouton constant, is directly related to the persistence length. The first reported experiments[13,14] suffered from two limitations in their interpretation:

1. The theoretical relation between the Cotton-Mouton constant and the persistence length had a wrong numerical factor, notwithstanding the need for more precise evaluation of the optical and magnetic anisotropy of the repeat unit, which enters as a proportionality factor.

2. The experiments were carried out at DNA concentrations of the order of $10^{-2}M$ in nucleotide, which implies that the contribution of the polymer to the screening of the electrostatic forces may become dominant at nominal concentrations of added salt $c_s < 10^{-2}M$. Therefore, the Cotton-Mouton constant seemed to become independent of c_s in the low-c_s region.

It is the purpose of this work to

a. reformulate the correct relation between the Cotton-Mouton constant and the persistence length,

b. discuss the improvements in the experimental setup that allowed us to extend the measurements to much lower c_p,

c. present the measurements of the Cotton-Mouton constant performed at different c_p as a function of c_s,

d. provide evidence for the existence of a master curve that describes the variation of the specific Cotton-Mouton constant as a function of a total effective ionic strength, including both c_p and c_s,

e. evaluate more thoroughly the optical and magnetic anisotropy, the latter from separate measurements, and

f. discuss the experimental dependence of the persistence length on ionic strength in comparison with recent measurements and in light of existing theories.

THEORY

Magnetic birefringence results from the orientation of molecules that are both magnetically and optically anisotropic by a strong magnetic field. As recognized by Wilson[15] for magnetic dichroism, calculation of the magnetic birefringence of chain molecules can be directly transposed from that of the electric birefringence when the orientation in the electric field is entirely due to an induced dipole mechanism, i.e., to the electric polarizability anisotropy. Substituting the electrical polarizability tensor α with the magnetic susceptibility tensor, χ, and the electric field, E, with the magnetic field, H, in the expression derived by Nagai and Ishikawa,[16] one gets the following for the birefringence (Δn) of a solution of molecules of molecular weight M at (mass-per-unit-volume-) concentration c_p,

$$\Delta n = \frac{2\pi}{n}\frac{N_a c_p}{M}\frac{1}{15}\left[3\langle \mathrm{Tr}\,\alpha_0\chi\rangle - \langle \mathrm{Tr}\,\alpha_0\,\mathrm{Tr}\,\chi\rangle\right]\frac{H^2}{2kT} \qquad (1)$$

where n is the index of refraction of the solution, N_a is Avogadro's number, α_0 is the optical polarizability tensor, and kT has the usual meaning.

Since locally the chains have a rather cylindrical symmetry, the Clausius-Mosotti correction for the internal field should not apply and all internal field corrections or form birefringence are included in the definition of α_0. This should be kept in mind when deriving the optical anisotropy from other optical experiments, such as electric or flow birefringence.

Introducing the traceless tensors, $\hat{\alpha}_0$ and $\hat{\chi}$, following Flory and Jernigan,[17] Eq. (1) can be written as

$$\Delta n = \frac{2\pi}{n}\frac{N_a c_p}{M}\frac{1}{10}\langle \mathrm{Tr}(\hat{\alpha}_0\hat{\chi})\rangle \frac{H^2}{kT} \tag{2}$$

An evaluation of the average trace has been carried out by Wilson[15] for a model of infinitely long and flexible helices. For the case where $\hat{\alpha}_0$ and $\hat{\chi}$ are axially symmetric with their axes along the chain direction, his result can be derived quickly using known properties of the wormlike model; it can also be extended to chains of arbitrary contour length, L, with respect to the persistence length, q. One simply has

$$\langle \mathrm{Tr}\,\hat{\alpha}_0\hat{\chi}\rangle = \frac{2}{3}\Delta\alpha_0\Delta\chi \sum_{i=1}^{N}\sum_{j=1}^{N}\left\langle\frac{3\cos^2\theta_{ij}-1}{2}\right\rangle \tag{3}$$

where $\Delta\alpha_0$ and $\Delta\chi$ are the difference between the longitudinal and transverse monomeric optical polarizabilities and magnetic susceptibilities, respectively; θ_{ij} is the angle between the axes of the tensors associated with monomers i and j. The double sum, which extends over all pairs i and j of the N monomers in the molecule, has been evaluated[18] in the framework of calculating the anisotropic light scattering of wormlike chains.

Neglecting all long-range correlations eventually resulting from excluded-volume interactions gives

$$\sum_i\sum_j\left\langle\frac{3\cos^2\theta_{ij}-1}{2}\right\rangle = N^2\frac{2q}{3L}\left[1-\frac{q}{3L}\left(1-\exp\left(-\frac{3L}{q}\right)\right)\right] \tag{4}$$

From Eqs. (2)–(4), introducing the monomeric length $l_0 = L/N$, and the monomeric molecular weight, m_0, one gets for the specific Cotton-Mouton constant,* defined as $\Delta n/c\lambda H^2$, where λ is the wavelength of the incident light

$$\frac{CM}{c_p} = \frac{\Delta n}{c_p\lambda H^2} = \frac{4\pi}{45}\frac{N_a}{\lambda n}\frac{1}{kT}\frac{\Delta\alpha_0\Delta\chi}{l_0 m_0}q\left[1-\frac{q}{3L}\left(1-\exp\left(-\frac{3L}{q}\right)\right)\right] \tag{5}$$

The bracketed term tends to 1 for $L \gg q$, so that for $L > 3q$, the expression becomes practically molecular-weight independent.

* Equation (5) is given in cgs units. In SI units it becomes

$$\frac{\Delta n}{c_p\lambda B^2} = \frac{1}{45}\frac{1}{\epsilon_0\mu_0}\frac{N_a}{\lambda_n}\frac{1}{kT}\frac{\Delta\alpha_0\Delta\chi}{l_0 m_0}q\left[1-\frac{q}{3L}\left(1-\exp\left(-\frac{3L}{q}\right)\right)\right]$$

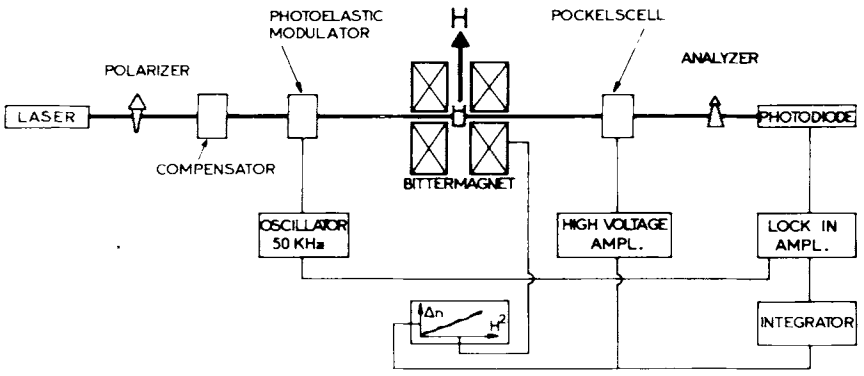

Fig. 1. Schematic representation of the experimental setup. Details are given in the text.

Magnetic birefringence appears, therefore, as a useful tool for the study of the persistence length, provided the product, $\Delta\alpha_0\Delta\chi$, can be obtained from separate experiments; all other terms being constant, the change of CM with ionic strengths in polyelectrolytes will directly reflect the changes in q.

Excluded-volume effects may introduce additional terms arising from long-range correlations between monomers at distances, $l_{ij} \gg q$, along the chain. While the change in end-to-end distance or radius of gyration with excluded-volume effects can be related to additional long-range terms in

$$\sum_i \sum_j \langle \cos \theta_{ij} \rangle$$

no direct calculation of this double sum or of Eq. (4) can be performed. From general arguments on the distribution of θ_{ij}, one can only expect that higher moments of the distribution will be less sensitive to small deviations from an isotropic distribution and that the higher-order average over a product of tensors will be less sensitive to excluded-volume interactions than the scalar product involved in the calculations of mean-square dimensions.

EXPERIMENTAL

Magnetic Birefringence

A sketch of the experimental setup is shown in Fig. 1. For clarity, some weakly focusing lenses and two pinholes are not shown. A vertical steady magnetic field, H, of up to 13.5 T (1.35×10^5 G) is produced by a water-cooled Bitter-type solenoid having an axial vertical bore (4.5-cm diameter), and two orthogonal radial 0.4-cm bores. The relative field variation over a sample of 3.0-cm optical path is smaller than 10^{-3}. A full sweep of the

magnetic field is usually performed within 60 s or less. A 0.5-T peak-to-peak amplitude modulation of frequencies between 0.5 and 2.5 Hz can be superimposed.

Laser light of various wavelengths (He-Ne, Ar, Kr, in this paper: $\lambda = 632.8$ nm) propagates horizontally through one of the radial bores; polarizer and analyzer (10-mm Glan-Thompson prisms) are crossed at 45° with respect to H. A photoelastic modulator[19] aligned with its optical axis parallel to H produces a sinusoidal variation of the phase difference, $\Delta\phi$, between the horizontally and vertically polarized light component at a frequency $\omega = 50$ kHz and an amplitude of $\Delta\varphi \sim 0.2\pi$. $\Delta\phi = \Delta\varphi \sin \omega t$. A photodiode output then occurs at 100 kHz (since the measured light intensity is proportional to $\sin^2\Delta\phi/2$, hence proportional to $\Delta\phi^2$ for small $\Delta\phi$.) In addition, a steady phase difference, $\Delta\phi_0 = \Delta\phi_m + \Delta\phi_{BC} + \Delta\phi_e$, arises from the magnetic birefringence ($\Delta\phi_m$) of the sample from the Babinet-Soleil compensator ($\Delta\phi_{BC}$) and from the stress on lenses or cell windows ($\Delta\phi_e$). Hence, the diode output is proportional: $\Delta\varphi^2 \sin^2\omega t + 2\Delta\varphi\Delta\phi_0 \sin \omega t + \Delta\phi_0^2$. The mixed signal at ω is detected phase-sensitively by a first lock-in amplifier. Its dc output, being proportional to $\Delta\varphi\cdot\Delta\phi_0$, is used as an error signal in a feedback loop involving a polarity-converting integrator, a high-voltage amplifier, and a longitudinal Pockels cell. As the birefringence, $\Delta\phi_p$, of the Pockels cell is proportional to the voltage applied across it, $\Delta\phi_0$ can thus be continuously compensated by $\Delta\phi_p$, i.e., $\Delta\phi_0 \cong -\Delta\phi_p$. The voltage at the Pockels cell is therefore proportional to the steady birefringence $\Delta\phi_0$. The compensator is set to minimize $\Delta\phi_{BC} + \Delta\phi_e$ before switching on the magnetic field. $\Delta\phi_m$ and Δn are related by $\Delta\phi_m/2\pi = \Delta n(l/\lambda)$, with l being the optical path-length of the sample cell. The time constant of the feedback loop is adjustable between ~1 ms and ~10 s, depending on the signal-to-noise ratio in Δn. Therefore, Δn can be monitored continuously during a field sweep and is plotted against H^2. Figure 2 shows two examples from DNA solutions. They belong to the largest and smallest CM constants, respectively, measured in this work. CM is deduced from the slope of the straight line obtained in these plots. Calibration is obtained in two independent ways: (1) by measuring the voltage across the Pockels cell for various settings of the calibrated Babinet-Soleil compensator and (2) by measuring Δn vs H^2 for liquids with well-known CM constants, such as benzene.

If a continuous measure of CM is desired, the magnetic field is set to a high value and weakly modulated (typically by $\Delta H/H \sim 5\%$) at a low frequency (~2.5 Hz). This results in an LF modulation of the compensating voltage of the Pockels cell; the amplitude of this LF signal is proportional to $H\Delta HCM$ and is monitored continuously using a second lock-in amplifier (not shown in Fig. 1). The experimentally determined resolution of the apparatus is about 10^{-10} in Δn, and 10^{-16} G^{-2} cm^{-1} in CM, using a sample length of $l = 3$ cm (sample volume about 1 mL) for transparent liquids. A measurement of Δn vs H^2 is performed typically within 5–10 min, including mounting and dismounting the sample cell. These improved specifications

were achieved essentially by a careful design of sample cells and holder: Teflon cells were used that were sealed with thin circular quartz plates by means of a thermoretractable plastic tube in order to minimize residual stress birefringence in the windows. The cells fitted tightly into a completely closed copper jacket having 0.2-cm holes in front of the windows. The temperature of this unit is electronically stabilized to a few hundredths of a degree during a field sweep.

The resolution of the apparatus is affected mainly by the following three factors: (1) A magnetic field-dependent shift in $\Delta\phi_0$ (at $\Delta\phi_m = 0$); this is mainly due to a slight mechanical distortion of the Bitter solenoid under field, resulting in the appearance of reflections of some of laser light of undefined polarization from the inner parts of the small horizontal bore. This baseline shift is obviously very sensitive to optical misaligment and varies slightly from cell to cell. It is measured on the pure solvent with a reproducibility corresponding to about $\pm 1 \times 10^{-10}$ in Δn. It is subtracted from the actual signal. (2) For field sweep times of 30 s, this baseline uncertainty is larger than the slow drift of $\Delta\phi_0$ caused by variations in the environmental temperature. (3) The noise in $\Delta\phi_0$ [see Fig. 2(b)] results mainly from mechanical vibrations of the optical elements, which are fixed on two separate optical benches of a total length of ~6 m. It can best be averaged out by performing several field sweeps. Points (1) and (3) are related to the use of Bitter magnets and should, in principle, not occur with superconducting solenoids or electromagnets. However, commercial superconducting coils with a radial optical axis usually still suffer from somewhat lower maximum fields ($\Delta n \sim H^2$), from additional (thick) windows substantiating the influence of residual stress birefringence, and, perhaps most importantly, from much lower field sweep rates. We expect the resolution-limiting factor then to be thermal baseline drifts. Special superconducting magnets could be designed to overcome these problems.

In electromagnets ($H \lesssim 2$ T), the lack of strong fields can be compensated by the possible use of long optical paths (meters!); because of the difficulty of proper light propagation over such long distances in polymeric liquids (Schlieren, etc.) and the requirement for large amounts of sample, these magnets are more suited to Cotton-Mouton studies on gases and simple liquids. The setup described here makes possible high-resolution Cotton-Mouton experiments on dilute solutions of (biological) materials available only in small amounts.

Sample Preparation

Lyophilized erythrocyte DNA (lot P671) was a kind gift of Dr. J. Pouyet, IBMC, Strasbourg. The average molecular weight was 4.2×10^6 as evaluated from the sedimentation coefficient s^0_{20w}. Water for solutions and for washing containers was distilled, deionized (resistivity ≥ 14 MΩ m), and filtered (0.6-μm pore size). Samples at $c_s \leq 10^{-3}M$ were kept between 0 and 4°C throughout the experiment. Pipettes, containers, optical cells,

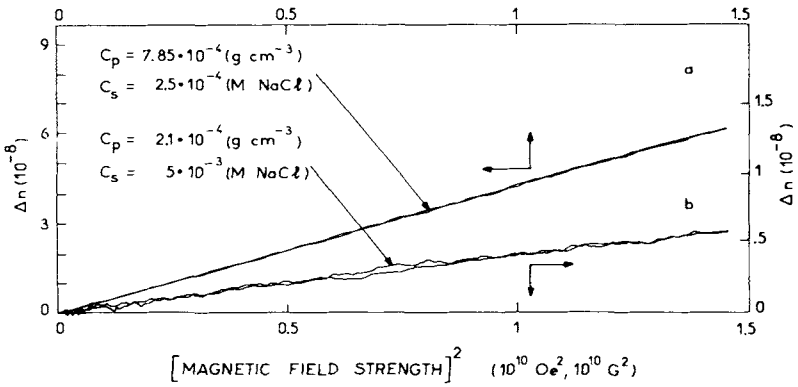

Fig. 2. Typical magnetic birefringence measurement (Δn vs H^2) of DNA solutions. DNA concentrations c_p and ionic strength c_s are such that (a) and (b) belong to the highest and lowest Cotton-Mouton constants measured, respectively. Note the different Δn scales for (a) and (b). Temperature, 4°C.

and so forth were usually cooled prior to contact with samples. This is necessary because of the ionic-strength dependence of the denaturation temperature of DNA. Lots of a stock solution (3 mL; ionic strength, c_s = 10^{-4} NaCl and c_p = 7.2 10^{-4} g cm^{-3}) were dialyzed (see Table I) twice for about 48 h each against various experimental ionic strengths in 1000 cm^3; the first dialyzing bath contained $10^{-5}M$ EDTA. A few intermediate ionic strengths and a few concentrations c_p down to 8×10^{-5} g cm^{-3} were prepared by mixing or dilution. The lots were divided into two parts of equal volume. One part (A) of each sample was used for the CM measurement, for a subsequent determination of c_p by uv absorbance in stoppered 1-cm cells without dilution (using an o.d.-c_p conversion factor of 2×10^{-3} o.d. g^{-1} cm^3), and for a thermal denaturation run. The other part (B) was kept without handling at 4°C. c_p and hyperchromicities, h at λ = 259 nm, of samples (A) and controls (B) were measured and compared with the stock solution in order to check for eventual denaturation. Whenever uv spectra or thermal denaturation runs indicated any measurable sign of partial denaturation, the corresponding point was disregarded. The data shown in Table I were derived from samples (A) and controls (B) with experimental h values between 0.37 and 0.41 (average, 0.396 ± 0.015), indicating the fair integrity of nonrejected samples.

RESULTS

Figure 2 shows two typical magnetic birefringence measurements. They can be compared with an earlier measurement (cf. Fig. 1 in Ref. 13) that had been taken at much higher concentrations (c_p = 10^{-2} g cm^{-3} and c_s = 0.15M NaCl) using a Bitter magnet without radial bores, additional mirrors (cf. Fig. 1 in Ref. 14), and standard spectrometer cells with l = 1 cm. The comparison clearly demonstrates the recent improvement in

TABLE I
Experimental Cotton-Mouton Constants (CM) at Various DNA Concentrations (c_p) and Ionic Strengths (c_s)

Ionic-Strength Adjustment	c_s of Dialysis Bath (M NaCl)	c_s Corrected for Donnan Effect (M)	c_p of (A) (o.d. units)	c_p of (B) (o.d. units)	CM (10^{-16} G^{-2} cm^{-1})
Direct dialysis	2.0	2.0	10.80	10.60	138
	0.05	0.0499	8.15	8.03	119
	0.01	0.0098	17.28	—	254
	0.001	0.00087	16.48	16.33	383
	0.001	0.00092	10.06	8.95	213
	0.001	0.00096	—	3.92	98
	0.0005	0.00039	16.73	16.14	393
	0.0005	0.00040	15.63	15.20	608
	0.0005	0.00040	15.43	—	567
	0.0005	0.00040	15.31	15.06	454
	0.0005	0.00040	15.07	—	505
	0.0005	0.00043	9.04	8.64	219
	0.0005	0.00044	7.97	—	287
	0.0005	0.00044	7.68	7.51	218
	0.0005	0.00045	6.35	—	217
	0.0005	0.00046	—	4.35	98
	0.0005	0.00047	3.87	3.71	105
	0.0005	0.00048	2.32	2.23	58

	0.00026	0.00019	15.07	—	541
	0.00026	0.00023	3.97	—	156
	0.00026	0.00023	3.52	3.79	139
	0.00025	0.00018	15.91	15.75	655
	0.00025	0.00018	15.70	15.08	700
	0.00025	0.00022	4.55	—	159
Dilution of DNA with dialysis bath[a]	0.01	0.0099	8.32	8.31	121
	0.005	0.0050	4.15	4.34	62
	0.001	0.00097	4.59	4.43	92
	0.0005	0.00044	8.29	8.35	194
	0.0005	0.00046	4.44	4.51	109
Mixing samples of similar c_p[b]	0.0035	0.0033	16.43	16.63	266
Dilution with H_2O[c]	0.0025	0.0025	4.12	4.07	74
Addition of conc. NaCl Solution	0.5	0.5	16.53	—	217
	0.1	0.099	15.31	—	221
	0.0011	0.00098	15.28	—	381
Direct dialysis	0.0005 $MgCl_2$	—	16.33	15.95	224
	0.0001 $MgCl_2$	—	16.27	15.78	256

[a] c_s approximately constant, c_p varied.
[b] c_p approximately constant, c_s varied.
[c] c_p c_s both varied.

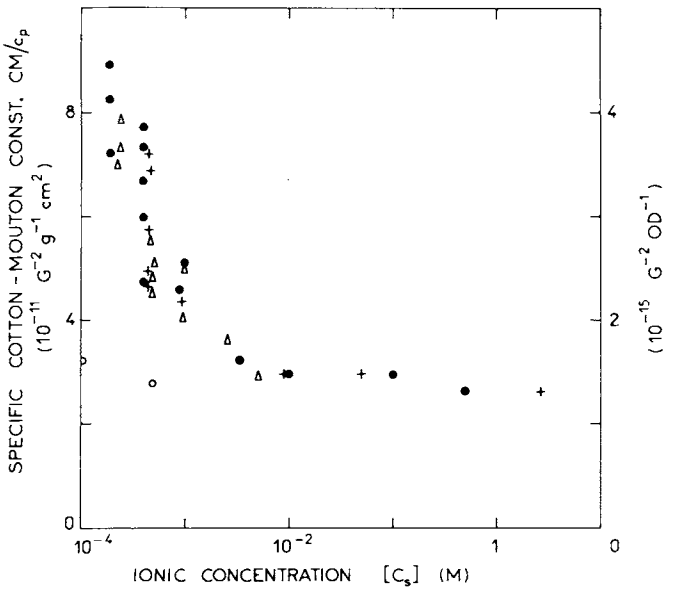

Fig. 3. Variation of the specific Cotton-Mouton constant CM/c_p of DNA in aqueous solution as a function of the concentration of additional salt, c_s, for several polymer concentrations c_p. The c_s values of the dialyzing bath (first column in Table I) were converted into the effective ionic strength (second column in Table I) of the sample by using Manning's formula (Ref. 38) for the Donnan effect. This correction is negligible for $c_s \geq 10^{-3}M$ and still small even at the lowest c_s and highest c_p values. Symbols: NaCl at c_p = 15–16.7 o.d. cm^{-1} (●), 6.3–10.7 o.d. cm^{-1} (+), and 2.3–4.5 o.d. cm^{-1} (△), and $MgCl_2$ at c_p = 16.3 o.d. (○).

resolution. The experimental CM values given in the last column of Table I are plotted in Fig. 3 as CM/c_p versus the ionic strength of additional salt, c_s. Note that the ionic strength is provided by (monovalent) NaCl except for two points measured with (bivalent) $MgCl_2$. Above 10^{-2}, CM/c_p is found to be essentially independent of both c_s and c_p; this—including the absolute value of CM/c_p—agrees well with a similar plateau observed earlier for calf thymus DNA.[14] Below $10^{-2}M$, CM/c_p increases strongly with a decreasing c_s of simple 1:1 electrolyte (NaCl), whereas the increase is strongly suppressed by the presence of $MgCl_2$ (with no NaCl).

DISCUSSION

Effective Ionic Strength and the Concept of Counterion Condensation

A similar increase of CM/c_p with decreasing NaCl concentration occurring between 10^{-2} and $10^{-3}M$ was found earlier.[14] However, these experiments were carried out at substantially higher c_p ($\sim 3 \times 10^{-3}$ g cm^{-3}), corresponding to $\sim 10^{-2}M$ PO_4, and, in contrast to Fig. 3, CM/c_p seemed to level off below $10^{-3}M$ NaCl. The comparison between the old and new

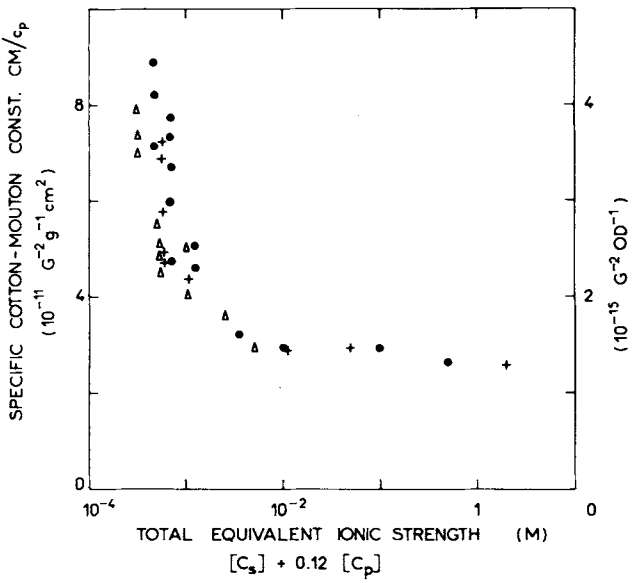

Fig. 4. CM/c_p values of Fig. 3 (except the two points with $MgCl_2$) plotted against an effective ionic strength $\mu_{\text{eff}} = c_s + (\alpha/2)c_p$ with $\alpha = 0.24$.

data thus strongly suggests a contribution of the counterions from the DNA phosphate groups to the total effective ionic strength. The leveling off at only $c_s \leq 10^{-3}M$ in the presence of $10^{-2}M$ PO_4 and $10^{-2}M$ corresponding counterions also seems to indicate that not all of the counterions dissociated from DNA should be numerically included in the effective ionic strength. We therefore tentatively express the effective ionic strength μ_{eff}, as the sum of c_s (corrected for the Donnan effect) and $(\alpha/2)c_p$, with $0 \leq \alpha \leq 1$, αc_p being the (molar) concentration of those dissociated counterions (with no corresponding co-ions) that play the same physical role as the Na^+ ions originating from c_s:

$$\mu_{\text{eff}} = c_s + \frac{\alpha}{2} c_p \tag{6}$$

(The factor 1/2 arises trivially from the definition of the ionic strength.) $\alpha < 1$ is actually consistent with the concept of counterion condensation.[20,21] In Manning's picture, it turns out that $1 - \alpha \cong 0.76$ of the counterions due to c_p are very close to the highly charged DNA surface (at room temperature). Thus, $\alpha \cong 0.24$ of the counterions contribute to long-range interactions. Therefore, we plot the experimental CM/c_p values vs μ_{eff} with $\alpha = 0.24$ (Fig. 4). A comparison with Fig. 3 shows that this procedure essentially shifts points below $\sim 10^{-2}M$ somewhat (though not much) to the right, the shift being proportional to c_p. At the present level of experimental scattering in this data, the points seem to be close to a c_p-independent master curve. It is noteworthy that a master curve cannot be

obtained that is compatible with the scatter in data from corresponding plots for $\alpha \geq 0.5$: an inverse systematic c_p dependence would then appear at $\mu_{\text{eff}} \leq 10^{-2}M$ (i.e., points with higher c_p become displaced significantly to the right of points with lower c_p). Therefore, these measurements, though indirectly and not in a very precise way, support the idea of counterion condensation.

Intrinsic Persistence Length of DNA at High Ionic Strengths

Before quantitatively interpreting our data in terms of intrinsic and electrostatic contributions to the persistence length with the aid of Eq. (5), we wish to insist on the observed *weak* relative variation of CM/c_p above $10^{-2}M$. This basically agrees with the observed "plateauing" of linear flow dichroism,[12] of the light-scattering radius of gyration,[22] and—as far as measured—of electric birefringence relaxation.[9] It contrasts, however, with the strong ionic-strength dependence of light-scattering data reported by Eisenberg and coworkers,[23] even when corrected differently[24] for excluded-volume effects. Recent flow-birefringence data[11] seem to show a weaker, though significant, salt dependence. We return to this comparison at the end of this paper.

What is known about $\Delta\alpha_0$ and $\Delta\chi$, the essential quantities (the other entries being well known) in Eq. (5) for determining an absolute q value?

Optical Anisotropy Factor $\Delta\alpha_0$

The optical anisotropy of one monomeric unit in double-helical DNA can be obtained by different experimental approaches:

1. From the birefringence of slightly oriented solutions, the degree of orientation being derived independently, for example, from simultaneous measurements of electric birefringence and dichroism; tilting of the base pairs is assumed to be known and generally put at zero.
2. From the birefringence of highly oriented solutions, where the molecules are simultaneously deformed into straight rods by an applied (electric) field; this is demonstrated by the molecular-weight-independent value of the specific electric birefringence of DNA solutions extrapolated to infinite field.
3. From the birefringence of highly oriented films or fibers of DNA.

The optical anisotropy is currently defined as the difference in polarizability per unit volume $(g_1 - g_2)$ or the difference in polarizability per base pair $\Delta\alpha_0$, which are linked by

$$\Delta\alpha_0 = (g_1 - g_2)(m_0\bar{v}/N_a) \tag{7}$$

where $\bar{v}$ is the (partial) specific volume. This relates to Δn_s of an ideally

oriented sample of parallel chains at concentration, c_p, by

$$\Delta n_s = \frac{2\pi}{n}(g_1 - g_2)\bar{v}c_p = \frac{2\pi}{n}\frac{\Delta\alpha_0}{m_0}c_p N_a \tag{8}$$

This relation between birefringence and optical anisotropy [Eqs. (7) and (8)] corresponds to the one used in Eqs. (1)–(5). $\Delta n/\Delta n_s$ can thus be considered as the degree of magnetic orientation.

The different values of $(g_1 - g_2)$ obtained from method (1) have been reviewed recently.[25] They all fit to within ±10% of the value $(g_1 - g_2) = -0.0215$ we obtained[26] using a combination of electric birefringence and electric dichroism of an intercalated dye. This latter value corresponds, using $m_0 = 690$ and $\bar{v} = 0.50$ cm^3/g, to $\Delta\alpha_0 = -12.5 \times 10^{-24}$ cm^3 or $\Delta n_s/c_p = -5.08 \times 10^{-2}$ g^{-1} cm^3. We repeat that the values for $\Delta\alpha_0$ and $(g_1 - g_2)$ include eventual local field corrections (or form birefringence) in the sense outlined in Eq. (1). The experimentally accessible quantity (which is the one relevant to this work) is $\Delta n_s/c_p$. The value obtained from the extrapolation to saturation of the electric orientation (2) is 30% higher $(g_1 - g_2 = -0.028)$.[25] Contrary to Stellwagen,[25] an ever higher value is obtained from the birefringence of a highly oriented fiber given by Seeds and Wilkins[27] ($\Delta n = -0.11$) if one takes into account the concentration of water inside the hydrated film required to preserve the B-form: Seeds and Wilkins estimate the water content of their samples to be about 30%, corresponding to about 43 wt % of H_2O per dry DNA; this is in good agreement with later accurate hydration measurements[28,29] on sodium DNA (43–46%). For their samples, this results in $c_p \simeq 1.08$ g cm^{-3} and in an average refractive index $n \simeq 1.53$ using $dn/dc = 0.188$ cm^3 g^{-1}. From Eq. (8) we thus obtain $(g_1 - g_2) = 0.049$. We have consistently found similar birefringence values (preliminary $\Delta n \sim -0.107$ g^{-1} cm^3) recently (G. Maret and G. Fillion, unpublished results) from oriented films of DNA in the A-, B-, and C-form, when corrected for base tilting and disorientation (of the crystalline regions) through an analysis of x-ray patterns.

A possible explanation for the comparatively high value found in fibers and films might be related to the difference in the internal field correction: from our definition of $\Delta\alpha_0$, which incorporates the anisotropy of the internal field and which is the measured quantity via Eqs. (7) and (8), it follows that

$$\Delta\alpha_0 = (\alpha_\parallel E_\parallel - \alpha_\perp E_\perp)/E_0$$

with $\alpha_\parallel$ and $\alpha_\perp$ being the intrinsic polarizabilities; E_0 is the incident electromagnetic field, and $E_\parallel$ and $E_\perp$ the internal field for E_0 directed along and perpendicular to the helix axis. It is known from the treatment of hypochromicity as a local field effect[30] that in solution, $E_\perp < E_\parallel$, so that, since $|\alpha_\perp| > |\alpha_\parallel|$,

$$|\Delta\alpha_0| < |\alpha_\parallel - \alpha_\perp|$$

The effect of internal field will be reduced when passing from the solution to the film because the polarizability of the surrounding medium approaches that of an individual DNA molecule.

A similar conclusion would be reached when treating the internal field effect as a form anisotropy: form anisotropy (Δn_f always > 0) opposes the intrinsic anisotropy ($\Delta n < 0$) and is less important in the fiber or film due to better index matching. In what follows, we will therefore assume $\Delta\alpha_0 = -12.5 \times 10^{-24}$ cm^3 for the solution, whatever its ionic strength, keeping in mind that this is probably a lower limit for a base-pair anisotropy. [Attributing the difference in Δn between films and solutions to form birefringence implies that $\Delta\alpha_0$ depends on the (ionic-strength-dependent) refractive index of the solvent. It can be estimated that the change in $\Delta\alpha_0$ amounts only to about 5% when going from pure water to 1*M* NaCl. Considering the scattering of our data points, we neglect this small correction, because it would not significantly change any conclusions.]

Diamagnetic Anisotropy Factor $\Delta\chi$

The diamagnetic anisotropy of DNA has not been extensively studied despite its importance for diamagnetic shielding effects in high-resolution nmr experiments. $\Delta\chi$ values have been estimated theoretically[31] for a number of aromatic bases and base pairs, with the results that the anisotropy of an A-T pair (G-C pair) exceeds that of benzene (-8.9 to -10.6×10^{-29} erg G^{-2}, as described in Ref. 32) by a factor of 1.098 and 0.827, respectively. Deriving $\Delta\chi$ of DNA from these numbers, as done in earlier work,[13] implies the assumption (1) of their correctness on an absolute scale and (2) of negligible contributions from other groups and bonds such as sugar and phosphate. Being unaware of experimental data in the literature, we have carried out susceptibility measurements with a sensitive SQUID-magnetometer on various oriented films of A-, B-, and C-DNA; these experiments will be published elsewhere (G. M. Fillion and G. Fillion). We propose that the experimental anisotropy seems to be substantially higher than the theoretical values suggested for the sole base pairs. A preliminary $\Delta\chi$ value for B-DNA would be $\Delta\chi = -17 \pm 3 \times 10^{-29}$ erg G^{-2} per monomer unit, resulting from averaging over different films and including corrections for base tilt in the A- and C-films and disorientation (of the crystalline regions). The given error represents only the statistical scattering in the data obtained so far. We believe—for several, essentially technical, reasons that cannot be outlined here—that the mean $\Delta\chi$ value should be considered as a slight underestimate of the true value for B-DNA.

Intrinsic Persistence Length of DNA

An absolute value of the intrinsic persistence length, q_p, is evaluated using Eq. (5). With the experimental CM/c_p value, 2.9×10^{-4} G^{-2} cm^2 g^{-1} in the plateau, $\Delta\alpha_0$ and $\Delta\chi$ as quoted above, $l_0 = 0.34$ nm, $L \sim 2 \times 10^3$

nm, $n = 1.33$, and $kT = 300 \times 1.38 \times 10^{-16}$ erg, we find $q_p = 67.0$ nm. Note that with these values, the bracket in Eq. (5) differs from one by less than 10^{-3}; hence, CM/c_p is essentially independent of L and directly proportional to q. The uncertainties in $\Delta\alpha_0$ and $\Delta\chi$ result in an error of about $\pm 30\%$ in q_p. This interval covers, as expected, values somewhat above the currently accepted 50 nm because somewhat underestimated values of $\Delta\alpha_0$ and $\Delta\chi$ were used. Encouraged by the numerical consistency found, we proceed to a discussion of the low-salt regime in terms of electrostatic persistence length.

Electrostatic Persistence Length of DNA

It is physically plausible that electrostatic contributions to q become important when the Debye-screening length becomes comparable to the intrinsic persistence length, q_p. Many experiments—such as the generally established square-root dependence of the intrinsic viscosity of polyelectrolytes on the concentration, c_s, of added salt[33]—corroborate this picture of electrostatic chain expansion. Older theories[34] of this effect did not agree with experiments and suffered from some ad hoc assumptions. More recent theories by Odijk[3,4] and Skolnick and Fixman[5] for a wormlike chain with line charge independently predicted the same variation of q with ionic strength: including counterion condensation—which was neglected in the first version of Odijk's paper—the relevant formulas are

$$q = q_p + q_e, \quad q_e = \frac{1}{4\kappa^2 Q Z^2} \tag{9}$$

with $Q = e^2/\epsilon kT$ being the Bjerrum length (0.7 nm in H_2O at 300 K), e the elementary charge, ϵ the dielectric constant of the solvent, Z the ionic valency, and $\kappa = \lambda_D^{-1} = 3.3\mu^{1/2}$ nm^{-1} the inverse Debye length, where the ionic strength, μ, is expressed in molar units. Note that for monovalent–monovalent salt (NaCl), μ numerically equals the molar salt concentration, c_s, whereas $\mu = 3c_s$ for monovalent–bivalent salt ($MgCl_2$).

Equation (9) reflects the hypothesis in Manning's condensation picture that the linear charge density, e/A, of DNA without condensation ($A = 0.17$ nm) is reduced, due to condensation, by a factor $\alpha = A/QZ$. There is no adjustable parameter for the calculation of q_e. Figure 5 shows a plot of q vs $\mu = \mu_{\text{eff}}$, using Eqs. (6) and (9) with $Z = 1$ (NaCl), compared with experimental data for four different values of q_p between 40 and 70 nm. This covers the range of uncertainty in q_p as derived from the plateau value of CM/c_p. In good agreement with our experimental data, the theoretical q value essentially levels off approaching q_p for ionic strengths above $10^{-2}M$ (NaCl). The agreement seems to persist also in the low-ionic-strength region (hence in total over about four orders of magnitude in μ_{eff}), where q_e rapidly becomes large for Na^+ counterions (cf. Fig. 5). For Mg^{2+}, q_e remains substantially smaller; the experimental values of $q = q_p + q_e$, as derived from Eq. (5) and $q_p = 60$ nm, are $q = 62$ nm and $q = 71$ nm at $c_s =$

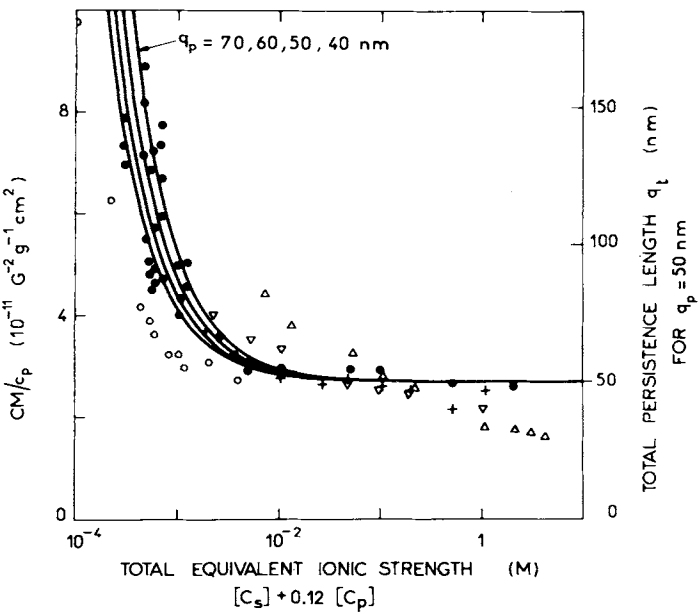

Fig. 5. Comparison of experimental values of the specific Cotton-Mouton constant (●) with theoretical values derived through a combination of Eqs. (5), (6), and (9) from the work of Odijk, Odijk and Houwaart, and Skolnik and Fixman (Refs. 3–5). The persistence length is expressed in units of the intrinsic value q_p, and the q_p values used cover a range consistent with the absolute plateau value of CM/c_p (see text). Various experimental q values taken from the literature are shown for comparison. They refer to a right-hand scale with q_p = 50 nm. Data: (○) electric birefringence relaxation (Ref. 9), (+) linear flow dichroism (Ref. 12), (▽) flow birefringence (Ref. 11), (△) light scattering (Ref. 23) corrected for excluded volume (Ref. 24).

5×10^{-4} and $10^{-4}M$ $MgCl_2$, respectively, these are in fair agreement with the theoretical values q = 65 nm and q = 77 nm calculated from Eq. (9) and using $\mu_{eff} = 3c_s + (\alpha/2)c_p$.

It should be kept in mind, however, that Eq. (9) is valid for $q_e < q_p$. In this sense, we can only say that the theory seems to describe well the onset of electrostatic contributions to q. A similar conclusion has also been drawn from an analogous Cotton-Mouton study[35] on solutions of polystyrene sulfonate (PSS), a substantially more flexible ($q_p \sim 1.2$ nm) polyelectrolyte; also, Eq. (9) does not incorporate excluded-volume effects, which might introduce both a chain expansion and orientation correlations in semidilute solutions. Excluded-volume effects are expected to become more important at low ionic strength. In fact, the rise of CM/c_p at low μ in PSS solutions was found to depend on the molecular weight.

For comparison, in Fig. 5 we have included Na^+-dependent q values as deduced from a number of other recent experiments on DNA; they are for various types of DNA with molecular weights ranging from $L \sim 170$ nm[22] to $L \sim 13.000$ nm.[11,12] A direct quantitative comparison is difficult because different techniques involve different scaling factors and different sensi-

tivities to excluded-volume effects, the latter certainly being important at the high L values and not always easily correctable. Despite this problem, all measures with the exception of the light-scattering data of Kam et al.[23] and perhaps the flow-birefringence data of Harrington[11] are consistent in revealing a plateau above $10^{-2}M$ NaCl with q_p values around 50 nm and a rise at lower μ. Unfortunately, not all measurements were extended to low μ in the regime of substantial stretching and more pronounced excluded-volume effects. Nevertheless, it is clear from Fig. 5 that the higher the L, the more pronounced the increase at low μ of—what we would like to call—the "apparent" q value. This seems to suggest that excluded-volume effects have not been properly accounted for in most of the experiments. They seem to be negligible only in the experiments of Hagerman[9] on restriction fragments ($L \sim 199.5$ nm) and of Mandel and Schouten[22] on sonicated DNA ($\bar{L} \sim 170$ nm). However, in this scheme the values of Rizzo and Schellman[12] should coincide with those of Harrington[11] ($L \sim 130.000$ nm in both experiments) rather than with our data ($L \sim 2.000$ nm). This and the inconsistency with Kam's data ($L \sim 21.700$ nm) indicate that other factors (which we presently ignore) might be involved.

CONCLUSION

New magnetic birefringence experiments, extended to DNA concentrations as low as 80 μg/mL and $2.5 \times 10^{-4}M < c_s$ (NaCl) $< 2M$, including recent experimental values for the monomeric optical and diamagnetic anisotropy, were used to derive an ionic-strength dependence of the persistence length, q, with the aid of a revised theoretical expression [Eq. (5)]. We find fair agreement with the theoretical prediction of Odijk[3,4] and Skolnick and Fixman[5] when counterion condensation is included following the concept of Manning. Our treatment disregards excluded-volume effects. Comparison of our results with those of others, however, indicates that these effects usually seem to become important at low ionic strength and have not been properly corrected so far. An evaluation of these corrections for the case of magnetic birefringence is interesting because it involves tensor averaging of optical and magnetic quantities that would also apply to the optical problem in flow birefringence and dichroism. We tend to believe (see Theory) that the correction should be small, but perhaps sufficient, to account for the discrepancy between our data and those of Hagerman.[9] The numerical agreement found between our uncorrected experimental q values and the theory (without excluded volume) could therefore be somewhat accidental in the low-ionic-strength region. This calls for additional magnetic birefringence data using DNA of widely different molecular weight. As pointed out by Fixman[5] and mentioned by Hagerman, introducing a finite DNA radius into the scaling theory could perhaps weaken the salt dependence, thus eventually reestablishing consistency. On the other hand, numerical calculations by Le Bret[36,37] that include a finite DNA radius yielded to a more sensitive salt dependence in the high-salt range, but this might be related to having neglected the

discrete nature of the charges, which becomes important when $\kappa^{-1} \sim A$ (M. LeBret, personal communication).

We are grateful to H. Dresler for substantial experimental assistance, to Dr. Pouyet for the kind gift of DNA samples, and to E. Senechal for stimulating discussions. Parts of the manuscript were written during G.M.'s stay at the Physics Department of the University of California at Los Angeles, and the financial support of Grant ONR N 00014-76-C-1078 is kindly acknowledged.

References

1. Roberts, R. J. & Murray, K. (1976) *CRC Crit. Rev. Biochem.* **4,** 123–144.
2. Sinsheimer, R. (1977) *Annu. Rev. Biochem.* **46,** 415–438.
3. Odijk, T. (1977) *J. Polym. Sci., Polym. Phys. Ed.* **15,** 477–483.
4. Odijk, T. & Houwaart, A. (1978) *J. Polym. Sci., Polym. Phys. Ed.* **16,** 627–639.
5. Skolnick, J. & Fixman, M. (1977) *Macromolecules* **10,** 944–948.
6. Schmid, C. W., Rinehart, F. P. & Hearst, J. C. (1971) *Biopolymers* **10,** 883–893.
7. Jolly, D. & Eisenberg, H. (1976) *Biopolymers* **15,** 61–95.
8. Rosenberg, A. H. & Studier, F. W. (1969) *Biopolymers* **7,** 765–774.
9. Hagerman, P. J. (1981) *Biopolymers* **20,** 1503–1535.
10. Ding, D. W., Rill, R. & van Holde, K. E. (1972) *Biopolymers* **11,** 2109–2124.
11. Cairney, K. L. & Harrington, R. E. (1982) *Biopolymers*, **21,** 923–934.
12. Rizzo, V. & Schellman, J. (1981) *Biopolymers* **20,** 2143–2163.
13. Maret, G., Schickfus, M. V., Mayer, A. & Dransfeld, K. (1975) *Phys. Rev. Lett.* **35,** 397–400.
14. Maret, G. & Dransfeld, K. (1977) *Physica* **86/88B,** 1077–1083.
15. Wilson, R. W. (1978) *Biopolymers* **17,** 1811–1814.
16. Nagai, K. & Ishikawa, T. (1965) *J. Chem. Phys.* **43,** 4508–4515.
17. Flory, P. J. & Jernigan, R. (1968) *J. Chem. Phys.* **48,** 3823–3824.
18. Arpin, M., Strazielle, C., Weill, G. & Benoit, H. (1977) *Polymer* **18,** 591–598.
19. Kemp, J. C. (1969) *J. Opt. Soc. Am.* **59,** 950–954.
20. Manning, G. S. (1969) *J. Chem. Phys.* **51,** 924–933.
21. Manning, G. S. (1979) *Acc. Chem. Res.* **12,** 443–449.
22. Mandel, M. & Schouten, J. (1980) *Macromolecules* **13,** 1247–1251.
23. Kam Z., Borochov, N. & Eisenberg, H. (1981) *Biopolymers* **20,** 2671–2690.
24. Manning, G. S. (1981) *Biopolymers* **20,** 1751–1755.
25. Stellwagen, N. C. (1981) *Biopolymers* **20,** 399–434.
26. Sokerov, S. & Weill, G. (1979) *Biophys. Chem.*, 161–171.
27. Seeds, W. E. & Wilkins, M. H. F. (1950) *Discuss. Faraday Soc.* **9,** 417–423.
28. Falk, M., Hartman, K. A., Jr. & Lord, R. C. (1962) *J. Am. Chem. Soc.* **84,** 3843–3846.
29. Rupprecht, A. & Forslind, B. (1970) *Biochim. Biophys. Acta* **204,** 304–316.
30. De Voe, H. (1964) *Biopolymers* **1,** 251–255.
31. Veillard, A., Pullmann, B. & Berthier, G. (1961) *C. R. Acad. Sci.* **252,** 2321–2322.
32. Battaglia, M. R. & Ritchie, G. L. D. (1977) *J. Chem. Soc. Faraday Trans. 2* **73,** 209–221.
33. Fuoss, R. M. & Strauss, V. P. (1949) *J. Polym Sci.* **3,** 602–604.
34. Chien, H. W., Isihara, C. & Isihara, A. (1976) *Polym. J.* **8,** 288–293.
35. Weill, G. & Maret, G. (1982) *Polymer* **23,** 1990–1993.
36. Le Bret, M. (1981) *C. R. Acad. Sci.* **292,** 291–294.
37. Le Bret, M. & Zimm, B. H. (1981) *Intermolecular Forces*, Pullmann, B., Ed., Reidel, Dordrecht, pp. 257–271.
38. Devore, D. I. & Manning, G. S. (1974) *Biophys. Chem.* **2,** 42–48.

Received January 20, 1983
Accepted April 18, 1983
Corrected proofs received November 26, 1983